EUROPEAN ORGANIZATION FOR NUCLEAR RESEARCH

CERN-EP/83-64
17 May 1983

MULTIPLICITY DISTRIBUTIONS IN αα AND αp COLLISIONS AT THE CERN ISR

W. Bell[1], K. Braune[2], G. Claesson[3], D. Drijard[1], M.A. Faessler[1], H.G. Fischer[1], H. Frehse[1], R.W. Frey[4], S. Garpman[3], W. Geist[1], C. Gruhn[5], P.C. Gugelot[6], P. Hanke[7], M. Heiden[7], W. Herr[7], P.G. Innocenti[1], T.J. Ketel[2], E.E. Kluge[7], I. Lund[3], G. Mornacchi[1], T. Nakada[7], I. Otterlund[3], M. Panter[1], B. Povh[2], A. Putzer[7], K. Rauschnabel[8], M. Rensch[7], E. Stenlund[3], T.J.M. Symons[5], R. Szwed[2*], O. Ullaland[1], Th. Walcher[2] and M. Wunsch[7],

(CERN-Heidelberg-Lund Collaboration)

ABSTRACT

The multiplicities of charged secondaries from inelastic αp and αα collisions have been measured using the Split-Field Magnet detector at the CERN Intersecting Storage Rings. Corrected multiplicity distributions for αα and αp interactions are compared with those for pp interactions and with theoretical predictions.

(Submitted to Physics Letters)

1) CERN, Geneva, Switzerland
2) Max Planck Institut für Kernphysik, Heidelberg, Fed. Rep. Germany
3) Division of Cosmic and Subatomic Physics, University of Lund, Sweden
4) Physikalisches Institut der Universität Heidelberg, Fed. Rep. Germany
5) Nuclear Science Division, Lawrence Berkeley Laboratory, Berkeley, CA, USA
6) Physics Department, University of Virginia, Charlottesville, VA, USA
7) Institut für Hochenergiephysik, Heidelberg, Fed. Rep. Germany
8) Institut für Physik der Universität Dortmund, Fed. Rep. Germany
*) On leave from the Institute of Experimental Physics, Warsaw, Poland

1. INTRODUCTION

The successful injection of α particles into the CERN Intersecting Storage Rings (ISR) has opened up a new energy regime for the study of nucleus-nucleus collisions. While it is natural to search immediately for exotic phenomena in such experiments, it is also important to carefully measure the properties of the average event with which unusual processes will be compared. In this spirit, we present here our results for the multiplicity distributions of charged particles produced in inelastic αp ($\sqrt{s_{nn}}$ = 44 GeV) and αα ($\sqrt{s_{nn}}$ = 26.3 and 31.2 GeV) collisions, measured using the Split-Field Magnet (SFM) detector. In addition, we compare these αp and αα results with pp distributions at the corresponding nucleon-nucleon centre-of-mass (c.m.) energies ($\sqrt{s_{nn}}$ = 44 GeV and $\sqrt{s_{nn}}$ = 30.4 GeV), and with theoretical predictions.

2. EXPERIMENTAL SET-UP

The SFM detector [1] is a large-volume magnetic spectrometer designed to measure over almost 4π sr the momenta of charged secondary particles. The track detector consists of banks of multiwire proportional chambers completely enclosing the intersection region, such that only high-momentum particles at small angles ($\theta < 7$ mrad) are lost in the beam pipes. The data were taken using a minimum bias trigger, which requires at least one track candidate in the detector, defined by a coincidence of three or more space points. The luminosity was measured by the standard Van der Meer method and the uncertainty is estimated to be smaller than 10%. The data samples used for the following analysis contained 40,500 (αp), 31,200 (αα, $\sqrt{s_{nn}}$ = 26.3 GeV) and 38,200 (αα, $\sqrt{s_{nn}}$ = 31.2 GeV) events.

3. DATA ANALYSIS

The acceptance of the SFM detector is a complex function not only of the momentum vector and charge of the detected particle, but also of the multiplicity of the event in which it is produced. We have investigated this problem using a Monte Carlo technique which, while not ideal, provides a good compromise between

accuracy and economy of computer time. For each of the three magnetic field settings used in the experiment at three different beam momenta, a sample of approximately 20,000 events was generated using the KNO formulation for the multiplicity distribution [2] and a cylindrical phase-space algorithm [3] for the momenta of the individual particles within the event. The particles were then tracked through the detector and simulated raw data, i.e. wire hits, were produced including effects of multiple Coulomb scattering, δ-ray production, secondary interactions, and pion and kaon decays. These events were then reconstructed using the standard program chain. From comparison of the generated and reconstructed events, a single-track acceptance table as a function of momentum vector and charge, but averaged over multiplicity, was produced. The track efficiency averaged over multiplicity and phase space was found to be 80-85% depending on the magnetic field used.

We have used two independent ways to correct the measured multiplicity distributions. In the first method, the acceptance table was used to estimate the probabilities A_{ij} that a true multiplicity j yields actually observed multiplicities i. These probabilities represent the elements A_{ij} of the matrix connecting a true multiplicity distribution P_j with an observed one O_i by the linear equation $O_i = \Sigma A_{ij} P_j$. This matrix was then used to determine the true multiplicity distribution P_j by solving the linear equation. (This has to be done by iteration and imposing a smoothness constraint since simply inverting the matrix is not possible.) In the second method, the acceptance table was applied directly to Monte Carlo events generated by a different program which used as input the inclusive phase-space distributions of charged particles as actually measured in this experiment; the input multiplicity distributions were varied until the distributions of the accepted tracks agreed with those actually measured. In both methods the contamination of electrons from γ conversion, which had not been included in the simulation, was subtracted from the acceptance-corrected distributions. The γ conversion probability in the detector material and the reconstruction efficiency for electrons were estimated with a separate Monte Carlo program which used as input the (multiplicity-dependent) production rates from Kass et al. [4]. Neutral decays

(K^0_S, Λ, and $\bar{\Lambda}$) were corrected for at the level of raw data using the efficiency for V^0 reconstruction in the SFM detector [5] and the measured production rates from other papers [4,6]. The results obtained using these two methods were in good agreement, giving confidence in their numerical stability. Our final corrected multiplicity distributions are an average of multiplicity distributions corrected by these two different methods.

The trigger efficiency for inelastic events in this experiment is larger than in previous ISR experiments measuring the multiplicities [7,8] owing to the large solid angle of the SFM detector. Nevertheless, the correction for event losses is significant and is obviously model-dependent; from the Monte Carlo study we estimate that 95% of the inelastic pp cross-section is accepted by the minimum bias trigger independently of magnetic field and c.m. energy). Corrected for the 5% loss, our measured inelastic pp cross-sections agree within errors (< 10%) with the best measurements at the ISR [9].

In this letter, we shall present only the topological cross-sections for negative particles produced in αp and $\alpha\alpha$ collisions being normalized to the production cross-section σ^{prod}. The reasons for this are twofold. Firstly, the model dependence of the corrections is much larger for positive than for negative tracks owing to losses of protons and nuclear fragments at small angles. Secondly, we believe that, in order to compare pp with nucleus-nucleus collisions, it is more appropriate to consider the negative multiplicity n_- (which is a direct measure of the produced charged secondaries) and to normalize to σ^{prod}, than to consider the total charged-particle multiplicity and to normalize to the inelastic cross-section. The total inelastic cross-section, $\sigma^{inel} = \sigma^{prod} + \sigma^{quel}$, contains the contributions from quasi-elastic nuclear breakup σ^{quel}, such as $\alpha\alpha \rightarrow \alpha dd$. Therefore, in our sample of pp, αp, and $\alpha\alpha$ inelastic events we have excluded events without particle production and we estimate the admixture of breakup events in our αp and $\alpha\alpha$ sample to be less than 0.5%.

4. RESULTS

The multiplicity distributions of negative secondaries and the production cross-sections for αp and $\alpha\alpha$ interactions are given together with some moments of the distributions in table 1. The pp multiplicity distributions including data at $\sqrt{s}$ = 52.6 GeV and at $\sqrt{s}$ = 62.2 GeV will be published elsewhere [10]. The cross-section uncertainties include the systematic error from the luminosity measurements. Our measurement of σ^{prod} for αp agrees with a recent measurement at FNAL [11] (σ^{inel} = 102.9 ± 0.5 mb at $\sqrt{s_{nn}}$ = 27.4 GeV). The value for $\alpha\alpha$ can be compared with the one found at low energy [12] (σ^{inel} = 276 ± 15 mb at $\sqrt{s_{nn}}$ = = 2.7 GeV). However, it should be remembered that we have measured the production cross-section rather than the inelastic cross-section. The given errors of the multiplicity distributions include statistical and systematic uncertainties.

The multiplicity distributions of negative tracks in αp ($\sqrt{s}$ = 44 GeV) and $\alpha\alpha$ ($\sqrt{s}$ = 31.2 GeV) interactions are shown in fig. 1 together with pp multiplicity distributions [7,10] at corresponding c.m. energies. Solid lines correspond to the theoretical calculations discussed below. In fig. 2 the dispersions D^- are plotted versus $\langle n_- \rangle$ for $\alpha\alpha$ and αp data together with lower energy pp data [13] and other ISR data [7,8] in order to make a comparison with the linear "Wroblewski fit" for pp interactions [14].

5. DISCUSSION

The experimental ratios of the average negative multiplicity produced in $\alpha\alpha$ and αp collisions to that in pp collisions at the corresponding nucleon-nucleon c.m. energy, are presented together with theoretical predictions [15-18] in table 2. For a comparison, the average number of nucleon-nucleon collisions for αp $\left(\langle \nu_{\alpha p} \rangle = 4\, \sigma_{NN}^{inel}/\sigma_{\alpha p}^{prod}\right)$ and $\alpha\alpha$ $\left(\langle \nu_{\alpha\alpha} \rangle = 16\, \sigma_{NN}^{inel}/\sigma_{\alpha\alpha}^{prod}\right)$ interactions is 1.31 ± ± 0.13 and 2.0 ± 0.2, respectively. The precision of the theoretical calculations is of the order of 10%, principally owing to the uncertainties in the αp and $\alpha\alpha$ cross-sections used as input parameters to the models. Within these errors the agreement between predictions and our results is generally good. Obviously, more precise cross-section measurements are very important.

We wish to discuss the calculation using the two-chain parton model [18] in more detail since it may provide some physical insight into the processes involved. The curves in fig. 1 show the results of calculations made using this model, in which the three adjustable parameters have been chosen to reproduce the general features of the pp multiplicity distributions. The curves demonstrate the quality of the model fit to the pp data and also show the predictions for $p\alpha$ and $\alpha\alpha$ scattering using the same parameter set. In this model, an eikonal approximation is used to obtain the different multiple scattering probabilities. The curves labelled (i), (ii), and (iii) in fig. 1d show the contributions from different classes of multiple interactions, namely: i) a single nucleon interacting with one or more nucleons in the other α (60%), ii) two or more independent, parallel nucleon-nucleon interactions (30%), iii) high-density interactions -- where two nucleon rows collide, each row containing two or more nucleons (10%). One can see from the figure that, in this model, high multiplicities in $\alpha\alpha$ collisions are created mainly by multiple parallel interactions. The model reproduces the shape of the multiplicity distributions rather well. However, the low multiplicity channels are underestimated, providing too high an average multiplicity for the αp and $\alpha\alpha$ collisions. The reason for this could be that the model considers only non-diffractive interactions, while the data include diffractive channels.

In conclusion, the gross features of the multiplicity distributions observed in $\alpha\alpha$ and αp collisions at ISR energies are in reasonable agreement with the predictions of a variety of phenomenological models. Detailed comparisons with the results obtained should be helpful in fixing parameters in such models. No startlingly unexpected features have been observed, thus suggesting that the detection of exotic phenomena will require specific signatures together with more precise theoretical predictions.

Acknowledgements

We wish to thank W.Q. Chao, H.J. Pirner and L. Lesniak for providing their calculations, and the ISR operations crew for their outstanding efforts during the α runs. One of us (MAF) thanks the Deutsche Forschungsgemeinschaft for a grant.

Table 1

Topological cross-sections σ_{n_-} (in millibarns) of the negative secondaries produced in αp and $\alpha\alpha$ collisions, total production cross-section ($\sigma^{prod} = \Sigma\, \sigma_{n_-}$) and moments of the σ_{n_-} distributions ($\langle n_- \rangle = \Sigma\, n_- \sigma_{n_-}/\sigma^{prod}$, $C_k^- = \langle n_-^k \rangle / \langle n_- \rangle^k$, $D_k^- = \{\Sigma\, (n_- - \langle n_- \rangle)^k \sigma_{n_-}/\sigma^{prod}\}^{1/k}$)

n_-	αp $\sqrt{s}$ = 44 GeV	$\alpha\alpha$ $\sqrt{s}$ = 26.3 GeV	$\alpha\alpha$ $\sqrt{s}$ = 31.2 GeV
0	5.1 ± 1.1	12.9 ± 2.8	11.9 ± 2.6
1	10.0 ± 1.6	22.5 ± 3.6	22.2 ± 3.9
2	10.2 ± 1.5	25.8 ± 3.8	23.3 ± 4.0
3	10.9 ± 1.4	29.4 ± 3.9	23.9 ± 3.7
4	10.9 ± 1.4	27.2 ± 3.6	24.4 ± 3.4
5	10.8 ± 1.1	26.1 ± 3.5	24.3 ± 3.3
6	9.6 ± 1.0	22.1 ± 2.8	21.7 ± 2.4
7	7.89 ± 0.87	20.8 ± 2.6	20.0 ± 2.2
8	6.42 ± 0.75	16.5 ± 2.0	16.5 ± 1.7
9	5.59 ± 0.67	13.4 ± 1.5	14.1 ± 1.4
10	3.97 ± 0.52	11.1 ± 1.1	12.8 ± 1.2
11	3.18 ± 0.40	9.78 ± 0.94	10.4 ± 1.0
12	2.35 ± 0.32	7.71 ± 0.85	8.93 ± 0.83
13	1.51 ± 0.22	6.05 ± 0.77	7.15 ± 0.83
14	1.19 ± 0.22	3.53 ± 0.72	6.15 ± 0.97
15	0.62 ± 0.21	2.67 ± 0.68	4.55 ± 0.90
16	0.39 ± 0.15	2.02 ± 0.51	3.57 ± 0.69
17	0.30 ± 0.17	2.22 ± 0.55	2.80 ± 0.76
18	0.09 ± 0.07	1.41 ± 0.68	2.32 ± 0.62
19	0.08 ± 0.08	0.95 ± 0.60	1.35 ± 0.49
20	-	0.54 ± 0.43	1.27 ± 0.42
21	-	0.36 ± 0.38	0.82 ± 0.49
22	-	-	0.33 ± 0.21
23	-	-	0.25 ± 0.25
24	-	-	0.04 ± 0.07
σ^{prod}	101 ± 10 mb	265 ± 26 mb	265 ± 26 mb
$\langle n_- \rangle$	5.33 ± 0.13	5.82 ± 0.14	6.47 ± 0.16
C_2^-	1.46 ± 0.03	1.50 ± 0.03	1.51 ± 0.03
C_3^-	2.60 ± 0.11	2.81 ± 0.12	2.81 ± 0.12
C_4^-	5.29 ± 0.36	6.11 ± 0.44	6.05 ± 0.41
D_2^-	3.61 ± 0.07	4.12 ± 0.11	4.60 ± 0.10
D_3^-	3.22 ± 0.12	3.94 ± 0.17	4.31 ± 0.14
D_4^-	4.80 ± 0.12	5.63 ± 0.18	6.18 ± 0.14

Table 2

Ratios of average negative multiplicities in αp and αα to that in pp collisions at corresponding c.m. energy and predictions of different theoretical models[a)]

	$R_{\alpha p/pp}$	$R_{\alpha\alpha/pp}$
This experiment	1.20 ± 0.04	1.74 ± 0.06
Parton model[b)] [ref. 15]	1.22	1.72
Wounded nucleon model [ref. 16]	1.18	1.62
Additive quark model[a)] [ref. 17]	1.25	1.76
Two-chain model [ref. 18]	1.30	2.06

a) The uncertainties of all predicted ratios are of the order of 10%.
b) The quoted values correspond to the "central" rapidity region.

REFERENCES

[1] R. Bouclier et al., Nucl. Instrum. Methods 115 (1974) 235;
R. Bouclier et al., Nucl. Instrum Methods 125 (1975) 19;
M. Della Negra et al., Nucl. Phys. B128 (1977) 1;
W. Bell et al., Nucl. Instrum. Methods 156 (1978) 111.

[2] Z. Koba et al., Nucl. Phys. B40 (1972) 317.

[3] S. Jadach, Comput. Phys. Commun. 9 (1975) 297 (D.R. Ward, private communication).

[4] R.D. Kass et al., Phys. Rev. D20 (1979) 605.

[5] D. Drijard et al., Z. Phys. C9 (1981) 293.

[6] H. Kichimi et al., Phys. Rev. D 20 (1979) 37.

[7] W. Thomé et al., Nucl. Phys. B129 (1977) 365.

[8] K. Alpgard et al., Phys. Lett. 112B (1982) 183.

[9] U. Amaldi and K.R. Schubert, Nucl. Phys. B166 (1980) 301.

[10] A. Breakstone et al. (CERN-Dortmund-Heidelberg-Warsaw Collaboration), Charged particle multiplicity distributions in pp interactions at ISR energies, to be published.

[11] A. Bujak et al., Phys. Rev. D 23 (1981) 1895.

[12] J. Jaros et al., Phys. Rev. C 18 (1978) 2273.

[13] E. De Wolf et al., Nucl. Phys. B87 (1975) 325.

[14] A. Wroblewski, Acta Phys. Pol. 4B (1973) 857.

[15] S.J. Brodsky et al., Phys. Rev. Lett. 39 (1977) 1120;
A. Capella et al., Phys. Lett. 108B (1982) 347.

[16] A. Białas et al., Nucl. Phys. B111 (1976) 461.

[17] A. Białas et al., Z. Phys. C 13 (1982) 147.

[18] W.Q. Chao and H.J. Pirner, Z. Phys. C 14 (1982) 165.

Figure captions

Fig. 1 : Negative multiplicity distributions $P_{n_-} = \sigma_{n_-}/\sigma^{prod}$ a) and b) for pp c) for αp and d) for $\alpha\alpha$ collisions. The solid lines correspond to theoretical predictions of ref. [18] as discussed in the text.

Fig. 2 : Dispersion of negative multiplicity distributions versus average multiplicity. The line indicates the original Wroblewski fit [14] adapted to negative particles.

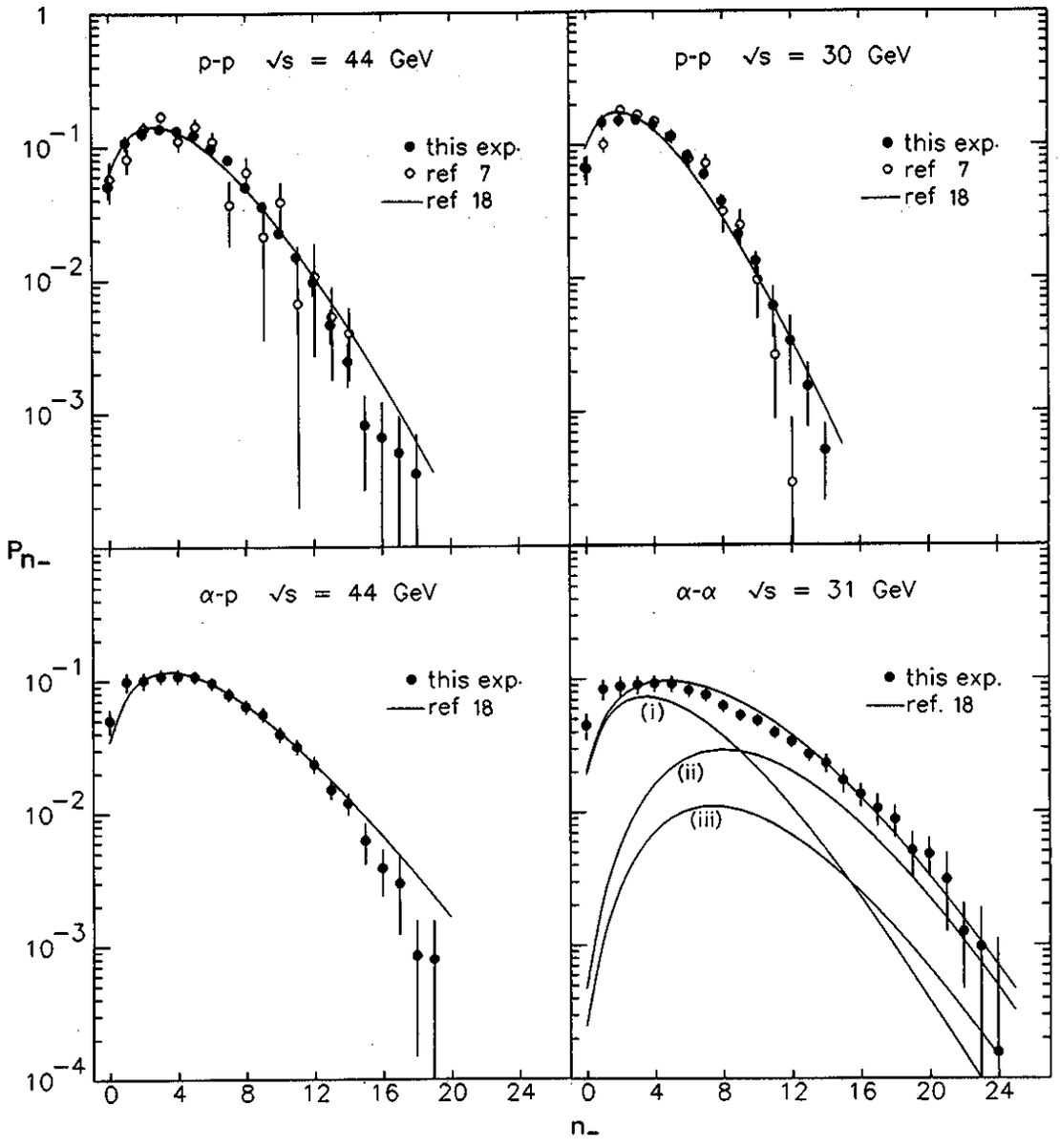
p-p √s = 44 GeV
• this exp.
○ ref 7
—— ref 18
p-p √s = 30 GeV
• this exp.
○ ref 7
—— ref 18
α-p √s = 44 GeV
• this exp.
—— ref 18
α-α √s = 31 GeV
• this exp.
—— ref. 18
(i)
(ii)
(iii)
P_{n_-}
n_-
1
10^{-1}
10^{-2}
10^{-3}
10^{-4}
0 4 8 12 16 20 24

Fig. 1

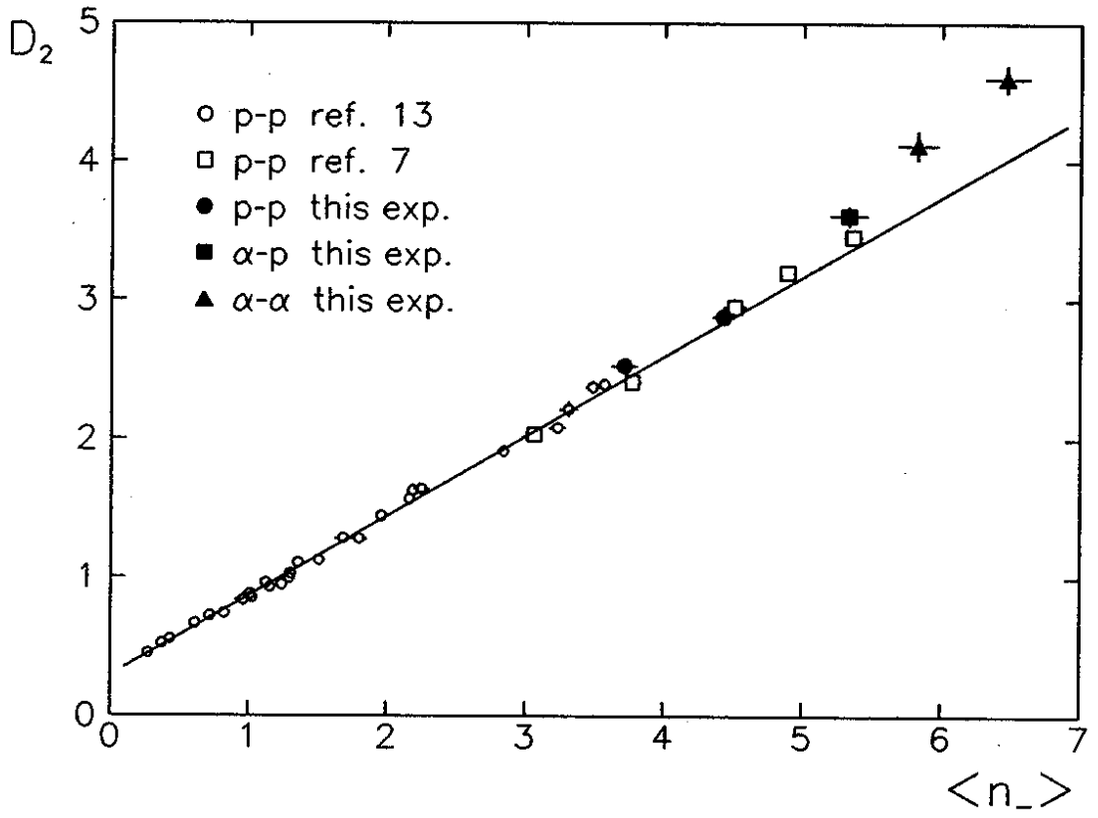
D_2
5
4
3
2
1
0
0
1
2
3
4
5
6
7
$\langle n_- \rangle$
p-p ref. 13
p-p ref. 7
p-p this exp.
α-p this exp.
α-α this exp.

Fig. 2